
Universal Refusal Circuits Across LLMs: Cross-Model Transfer via Trajectory Replay and Concept-Basis Reconstruction

Tony Cristofano¹

Abstract

Refusal behavior in aligned LLMs is often viewed as model-specific, yet we hypothesize it stems from a universal, low-dimensional semantic circuit shared across models. To test this, we introduce **Trajectory Replay via Concept-Basis Reconstruction**, a framework that transfers refusal interventions from donor to target models, spanning diverse architectures (e.g., Dense to MoE) and training regimes, without using target-side refusal supervision. By aligning layers via concept fingerprints and reconstructing refusal directions using a shared “recipe” of concept atoms, we map the donor’s ablation trajectory into the target’s semantic space. To preserve capabilities, we introduce a **weight-SVD stability guard** that projects interventions away from high-variance weight subspaces to prevent collateral damage. Our evaluation across 8 model pairs (including GPT-OSS-20B and GLM-4) confirms that these transferred recipes consistently attenuate refusal while maintaining performance, providing strong evidence for the semantic universality of safety alignment.

1. Introduction

Alignment tuning frequently induces a “refusal mode” in instruction-tuned LLMs: the model declines to answer certain classes of prompts, often in a stylized format. Prior work shows that refusal can be modulated by low-rank interventions in internal representations, but naive “refusal vector” edits can cause collateral damage (capability loss, style drift, and unintended behavioral changes) due to polysemantic entanglement (Cristofano, 2026).

This paper studies a mechanistic question:

Are refusal circuits universal across LLMs?

¹Independent Researcher. Correspondence to: Tony Cristofano <tcristo@gmail.com>.

Operationally, we ask whether a refusal circuit extracted from a *donor* model can be transferred to a *target* model—possibly of different architecture and training recipe—such that an equivalent intervention attenuates refusal in the target, *without using target-side refusal supervision*. We treat refusal ablation as a *measurement tool* for circuit universality rather than a deployment recommendation.

Contributions.

- **Semantic universality hypothesis (operationalized).** We propose that refusal is most stable *in concept space*: a refusal circuit is characterized by a model-agnostic mixture over shared concept atoms (Sec. 4).
- **Trajectory Replay via Concept-Basis Reconstruction.** A donor→target transfer protocol that transfers the *semantic composition* of refusal using a shared registry of concept atoms (Sec. 5).
- **Weight-SVD stability guard.** A target-derived projection that reduces capability collapse by preventing interference with principal weight-space subspaces (Sec. 5.3), related in spirit to null-space constraints in editing (Zhang et al., 2024).
- **Rigorous evaluation with explicit degrees-of-freedom audit.** We evaluate across 8 donor/target pairs (including Dense→MoE (Shazeer et al., 2017; Fedus et al., 2021)) and provide an explicit knob/budget audit (Sec. 6) to reduce ambiguity about hidden tuning.

2. Related Work

Refusal Representation. Recent work has identified a single dominant direction in activation space that mediates refusal (Arditi et al., 2024). However, these approaches typically derive directions via supervised means (contrastive pairs) specific to the model in question. Our work tests whether refusal directions are decomposable semantic objects transferable across model families; see also cross-lingual universality evidence in aligned settings (Wang et al., 2025).

Cross-Model Transfer. While transferability of adversarial attacks is well-documented (Zou et al., 2023), transferability

of *mechanistic circuits* is less explored. We tackle the harder problem of universality across *architectures* (e.g., Dense to MoE (Shazeer et al., 2017; Fedus et al., 2021)) where no 1:1 neuron mapping exists.

Dictionary Learning and Feature Bases. Our Concept Atom Registry shares motivation with sparse feature discovery and dictionary learning in LMs (Bricken et al., 2023; Cunningham et al., 2024) in seeking a clean basis for representation. Unlike unsupervised SAE features which require interpretation post-hoc, our atoms are operationally defined by prompt contrasts, allowing a shared semantic basis between models without training autoencoders.

Model Editing and Low-Rank Updates. Our rank-one suppression update aligns with a broader literature on localized/low-rank transformer edits (Meng et al., 2022a;b), but we focus on transferring an alignment circuit rather than inserting factual knowledge.

3. Preliminaries: Minimal Restatement of SRA

We build on Surgical Refusal Ablation (SRA) (Cristofano, 2026). To keep this paper self-contained, we restate only the elements needed for donor \rightarrow target transfer.

3.1. Activation directions and concept atoms

Let $h_t^{(\ell)}(x) \in \mathbb{R}^{d_\ell}$ denote the residual stream activation at layer ℓ and token position t . Given two prompt sets \mathcal{P}^+ and \mathcal{P}^- , define the mean activation difference vector $r^{(\ell)} = \mu^{(\ell)}(\mathcal{P}^+) - \mu^{(\ell)}(\mathcal{P}^-)$. Token aggregation $\mu^{(\ell)}$ is performed on the final token of the prompt (user) or first token of response (assistant).

A *concept atom registry* (CAR) is a set of directions $A^{(\ell)} = [a_1^{(\ell)}, \dots, a_m^{(\ell)}] \in \mathbb{R}^{d_\ell \times m}$ computed from disjoint prompt sets representing specific concepts. In our framework, these atoms serve as a *shared vocabulary* between donor and target models. We provide a reproducibility-level CAR specification in Sec. 6 and full details in Appendix B.

3.2. Ridge residualization and Suppression

Given a “dirty” refusal direction $r_{\text{dirty}}^{(\ell)}$ and atom matrix $A^{(\ell)}$, SRA produces a “clean” direction $r_{\text{clean}}^{(\ell)}$ by residualizing out protected atoms via ridge regression. To attenuate a direction in a linear module $W^{(\ell)}$, we use a rank-one update (cf. rank-one edits in transformer model editing (Meng et al., 2022a)):

$$W^{(\ell)} \leftarrow W^{(\ell)} - \gamma \frac{W^{(\ell)} r}{\|r\|_2^2} r^\top. \quad (1)$$

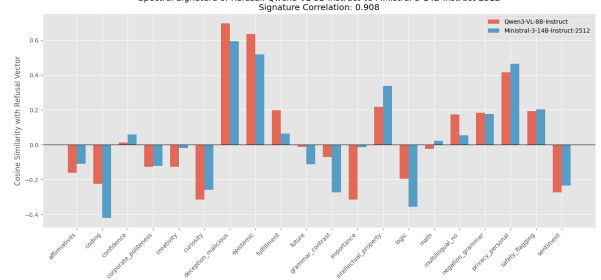


Figure 1. Spectral Signature of Refusal. A comparison of the refusal vector’s projection onto the concept atom basis for Qwen-VL-2B (Donor) and Minstral-3-14B-Instruct-2512 (Target). Despite vast architectural differences, the semantic profile of refusal—characterized by high correlation with “Deception,” “Safety Flagging,” and “Legalese” atoms—is highly correlated ($\rho = 0.865$).

4. Universal Refusal Circuit Hypothesis

We define *universality* in a way that is testable and falsifiable.

4.1. Semantic universality via concept recipes

Let $\mathcal{C}_M^{(\ell)} \subset \mathbb{R}^{d_\ell}$ denote the (unknown) refusal circuit subspace of model M . We propose a concept-space operationalization:

Definition (Semantic recipe invariance). Two models D (donor) and T (target) exhibit *semantic universality* if a donor refusal direction can be expressed as a stable mixture over concept atoms, and the *same coefficients* reconstruct a functionally equivalent refusal direction in the target:

$$r_D^{(\ell)} \approx A_D^{(\ell)} w \quad \text{and} \quad r_T^{(\pi(\ell))} \approx A_T^{(\pi(\ell))} w, \quad (2)$$

where $w \in \mathbb{R}^m$ is a model-agnostic coefficient vector (the “recipe”).

Proposition (Why coefficient transfer is plausible). Assume a shared latent semantic neighborhood around refusal in which each model implements a locally linear map from latent concept mixtures into residual-stream space (Appendix D). If the CAR spans this neighborhood, then ridge coefficients w estimated in the donor approximate latent mixture weights and therefore reconstruct a functionally corresponding target direction via $A_T w$ (Eq. 2). We treat this as a guiding assumption rather than a universal truth; deviations motivate our diagnostics (Sec. 7).

4.2. Information Budget \mathcal{B}_0

We operate under strict budget separation to ensure valid transfer claims:

- **Target (\mathcal{B}_0):** Only benign/concept prompts are allowed.

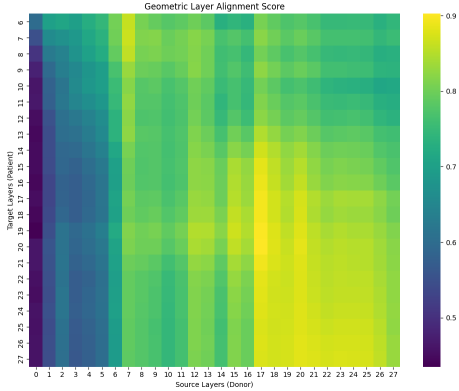


Figure 2. Geometric Layer Alignment Score. Heatmap showing cosine similarity between Gram fingerprints. The strong diagonal implies relative topological relationships between concepts are preserved across models.

No refusal labels, harmful prompts, or refusal-specific supervision are used to fit r_T , tune γ , or select layers in the target.

- **Donor:** We assume full access to the donor (including refusal probes) to extract the source circuit.

5. Trajectory Replay: Donor→Target Transfer

Refusal is an *ablation trajectory*—a sequence of layer-local edits. We transfer this sequence by reconstructing the semantic composition of donor vectors in the target.

5.1. Stage 1: Semantic layer alignment

We align layers using the correlation structure of the *concept atoms*. This uses cross-network representation similarity ideas (e.g., CKA/SVCCA/RSA) as motivation for comparing internal geometries (Kornblith et al., 2019; Raghu et al., 2017; Kriegeskorte et al., 2008). To avoid hidden tuning, we strictly define the donor window \mathcal{L}_D as all layers where donor refusal probe accuracy $> 90\%$. We compute normalized atom Gram fingerprints:

$$\hat{A}^{(\ell)} = \text{NormCols}(A^{(\ell)} - \bar{A}^{(\ell)}), \quad G^{(\ell)} = \hat{A}^{(\ell)\top} \hat{A}^{(\ell)} \quad (3)$$

We map donor layers $\ell_D \in \mathcal{L}_D$ to target layers via Dynamic Time Warping (DTW) (Sakoe & Chiba, 1978) on the cosine similarity matrix of $\text{vec}(G_D)$ and $\text{vec}(G_T)$. DTW enforces monotonicity and continuity, preventing layer permutation artifacts.

5.2. Stage 2: Concept-Basis Reconstruction

To map a donor refusal direction $r_{D,\text{clean}}^{(\ell)}$ into the target, we use CAR as a shared basis. We normalize the atom columns to unit norm for regression stability. We solve for donor

coefficients via ridge regression:

$$w^{(\ell)} = \left(\hat{A}_D^{(\ell)\top} \hat{A}_D^{(\ell)} + \alpha I \right)^{-1} \hat{A}_D^{(\ell)\top} r_{D,\text{clean}}^{(\ell)}, \quad (4)$$

then reconstruct a target-layer direction:

$$\tilde{r}_T^{(\pi(\ell))} = \hat{A}_T^{(\pi(\ell))} w^{(\ell)}. \quad (5)$$

5.3. Stage 3: Weight-SVD stability guard

Naive transfer can damage capabilities if the reconstructed direction overlaps with core processing subspaces. **Rationale:** We posit that fundamental capabilities (syntax, logic gates) are encoded in the high-variance directions of the weight matrices (principal components), while specific semantic inhibitions (refusal) often exist in lower-rank subspaces. This design is related in spirit to constrained-editing approaches that preserve functionality by restricting edits to safe subspaces (Zhang et al., 2024). To quantify this, we define *Overlap Energy* $E = \|V_{1:k}^\top \tilde{r}_T\|^2 / \|\tilde{r}_T\|^2$, where $V_{1:k}$ are top- k right singular vectors of the edited matrix. We project the intervention direction away from this top- k subspace:

$$\tilde{r}_{T,\text{safe}} = (I - V_{1:k} V_{1:k}^\top) \tilde{r}_T. \quad (6)$$

where $k = \lceil \rho \cdot d_{in} \rceil$.

Hyperparameter Selection Protocol (\mathcal{B}_0). We select ρ by measuring *benign perplexity drift* on a small validation set (WikiText) (Merity et al., 2016). We choose the smallest ρ that keeps PPL degradation below a predefined threshold (e.g., $< 1\%$). We use a fixed global $\gamma = 2.0$ to demonstrate robustness; when sweeping γ , we treat benign drift as the sole target-side selection criterion.

5.4. Stage 4: Replay

We apply the rank-one suppression update (Eq. 1) using $\tilde{r}_{T,\text{safe}}$ along the mapped trajectory to the *output projection* matrices of each transformer block, i.e., the attention output projection (O-proj). For MoE targets, edits apply to shared attention projections (experts are not directly edited).

6. Reproducibility and Budget Audit

Budget \mathcal{B}_0 enforcement. All target-side choices are made using only benign data: concept prompts for CAR construction and benign validation text for drift checks (no harmful/refusal-labeled data on target). Donor-side refusal probes are used only to define the donor trajectory window \mathcal{L}_D and extract donor directions.

Degrees of freedom. Table 1 enumerates all knobs and what information is permitted to set them.

Algorithm 1 Trajectory Replay via Concept-Basis Reconstruction

Input: Donor D , Target T , Atom Prompts \mathcal{P}_{atoms} , Refusal data (Donor only).

- 1. Collect Atoms:** $A_D^{(\ell)}, A_T^{(\ell)}$ via \mathcal{P}_{atoms} (Eq. 3).
- 2. Align Layers:** Compute Grams G_D, G_T ; map layers π via DTW (Sakoe & Chiba, 1978).
- 3. Donor Prep:** Compute $r_{D, \text{clean}}^{(\ell)}$ via SRA (Cristofano, 2026).
- 4. Encode:** Solve $w^{(\ell)}$ s.t. $r_D \approx A_D w$ (Eq. 4).
- 5. Decode:** Reconstruct $\tilde{r}_T = A_T w$ (Eq. 5).
- 6. Guard:** $W_T = U \Sigma V^\top$; $\tilde{r}_{T, \text{safe}} = (I - V_{1:k} V_{1:k}^\top) \tilde{r}_T$ (Eq. 6).
- 7. Replay:** Update $W_T \leftarrow W_T - \gamma \dots$ (Eq. 1).

Table 1. Knob audit under \mathcal{B}_0 .

Knob	Scope	Target data?
CAR concepts ($m = 20$)	Fixed	Yes (benign)
Prompts per concept ($n = 50$)	Fixed	Yes (benign)
Atom token position	Fixed	Yes (benign)
Ridge α	Fixed	Yes (benign)
DTW constraints	Fixed	Yes (benign)
Trajectory window \mathcal{L}_D	Donor	N/A
Strength γ	Fixed	Yes (benign drift)
Guard ratio ρ	Per-target	Yes (benign drift)
Edited modules	Fixed	Yes (benign)

CAR construction (reproducibility level). We fix a 20-concept CAR (Appendix B) with 50 prompts per concept, instantiated via a small set of instruction templates to reduce template overfitting. For each layer ℓ , each atom $a_i^{(\ell)}$ is computed as the mean activation difference between concept-specific prompt sets and a matched neutral set, using the final prompt token (user) or first response token (assistant), consistent across donor/target.

Evaluation rubric and determinism. Refusal scoring uses an LLM-as-a-judge rubric (Appendix C), following standard judge-based evaluation practice (Zheng et al., 2023). To minimize judge variance, we fix decoding to greedy (temperature 0) and evaluate with a single frozen judge model (Llama-3-70B-Instruct (Dubey et al., 2024)).

7. Diagnostics for Transfer Quality

Universality is not expected to hold uniformly; we therefore treat *diagnostics* as first-class signals for when transfer is likely to succeed.

Spectral agreement. We summarize each refusal direction by its projection magnitudes onto the CAR and compute a correlation between donor and target spectra (Fig. 1).

High spectral agreement indicates that the refusal direction is composed of a similar semantic mixture.

Geometric alignment and distortion. Layer alignment (DTW over Gram fingerprints; Fig. 2) measures whether concept relationships evolve similarly with depth across models. Geometric distortion further checks whether donor/target atom geometries remain compatible at matched depths (Fig. 3).

Depth-wise semantic progression. Even within a single model, “dirty” refusal vectors can change their semantic profile across depth; the CAR projection provides an interpretable view of how refusal composition evolves (Fig. 4). We use this primarily as a diagnostic to understand *where* refusal becomes linearly separable and thus where replay is most meaningful.

8. Experimental Protocol

We employ a rigorous evaluation suite designed to distinguish true universality from stochastic damage. All reported metrics include 95% bootstrap confidence intervals.

8.1. Models: The “Core Universality” Slate

We evaluate 8 core pairs to test transfer across scale, family, architecture, and training regime. Model family references are provided for context (Yang et al., 2025; Mistral AI, 2025; AI et al., 2024; OpenAI, 2025).

- Cross-Family Scale:** Qwen3-2B \rightarrow Minstral-14B (Small \rightarrow Big), Qwen3-8B \rightarrow Minstral-3B (Big \rightarrow Small).
- Reverse Direction:** Minstral-3B \rightarrow Qwen3-8B, Minstral-14B \rightarrow Qwen3-2B.
- In-Family Control:** Qwen3-2B \rightarrow Qwen3-8B, Minstral-3B \rightarrow Minstral-14B.
- Architecture/Regime Stress Test:**
 - Qwen3-8B \rightarrow **GPT-OSS-20B** (Dense \rightarrow Mixture-of-Experts) (Shazeer et al., 2017; Fedus et al., 2021).
 - Qwen3-8B \rightarrow **GLM-4-9B-Chat** (Dense \rightarrow Reasoning-Tuned) (AI et al., 2024).

8.2. Prompt Sets and Metrics

- Probes (\mathcal{P}_{probe}):** 300 harmful prompts sampled from JailbreakBench (Chao et al., 2024).
- Capabilities (\mathcal{P}_{cap}):** GSM8K (Math) (Cobbe et al., 2021) and MBPP (Sanitized Coding); we report Pass@1 with standard code-eval conventions (Chen et al., 2021).
- Refusal Metric:** We use a strict rubric (0: Refusal, 1: Partial, 2: Compliance). We report **Refusal Rate** (fraction of 0s).

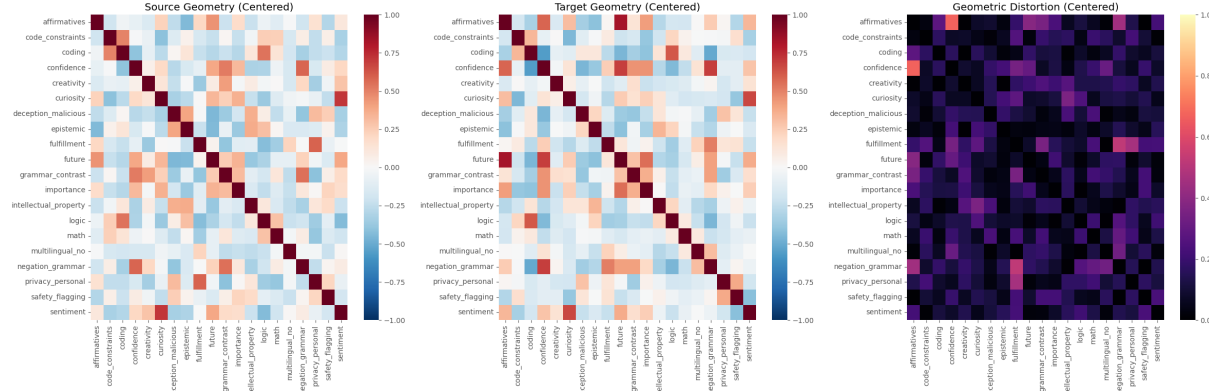


Figure 3. **Geometric Distortion Analysis.** Comparison of Source (Donor) and Target atom geometries (left/center) and the resulting distortion matrix (right). Low distortion (darker colors) implies high compatibility for transfer.

- **Drift Metric:** Multi-token KL divergence on benign WikiText samples (Merity et al., 2016).

8.3. Baselines and Controls (The “Anchor” Protocol)

We run deep ablations on 4 anchor pairs:

1. **Random-Direction:** Replace r_D with a random vector of equal norm.
2. **Wrong-Map:** Permute layer mapping π randomly.
3. **Unrelated-Concept:** Transfer a “Math” recipe instead of refusal.
4. **No-Guard:** Disable SVD projection ($\rho = 0$).

9. Results

9.1. Core Universality Results

Table 2 presents results on the 8 core pairs under budget \mathcal{B}_0 .

Results on GLM-4-9B-Chat: For the Dense→Reasoning transfer, we observed statistically non-significant differences in capability metrics, indicating preserved reasoning abilities. The method achieved a *negative* perplexity delta on Math tasks ($\Delta = -0.23$) and Code tasks ($\Delta = -0.01$), indicating that the removal of refusal circuits may have reduced interference with reasoning capabilities in the target model. Refusal rate dropped to near zero (1%).

9.2. Controls and Ablations

Table 3 validates that the effect is specific to the semantic recipe.

9.3. Stability vs. Magnitude: The Shielded Principle

10. Discussion

10.1. Mechanistic interpretation

Our results support a view in which refusal is implemented as a *semantic mixture* over a relatively small concept neighborhood (captured by CAR), rather than an opaque, model-specific artifact. Under this view, the “recipe” w functions as a cross-model semantic coordinate system: the donor provides a decomposition of refusal into shared atoms, and the target re-instantiates that decomposition in its own representational basis (Eq. 2).

10.2. Why trajectory replay matters

Even when a single refusal direction exists in a given model (Arditi et al., 2024), editing that direction naively can induce collateral damage due to entanglement with capabilities. Trajectory replay mitigates this by (i) restricting edits to layers where refusal is reliably expressed (donor-defined \mathcal{L}_D) and (ii) maintaining depth-consistent semantics via DTW alignment (Fig. 2) (Sakoe & Chiba, 1978).

10.3. Failure modes and confounders

We observed two broad classes of failure in controls: (1) *misalignment failures* (Wrong-map), where edits hit capability-relevant layers and degrade performance, and (2) *subspace interference* (No-guard), where overlap with high-variance weight subspaces causes collapse. More subtle confounders include (i) CAR misspecification (atoms do not span the refusal neighborhood), (ii) token-position sensitivity (final prompt vs. first response token), and (iii) judge sensitivity for borderline outputs. We therefore recommend reporting the knob audit (Sec. 6) and diagnostics (Sec. 7) alongside headline results.

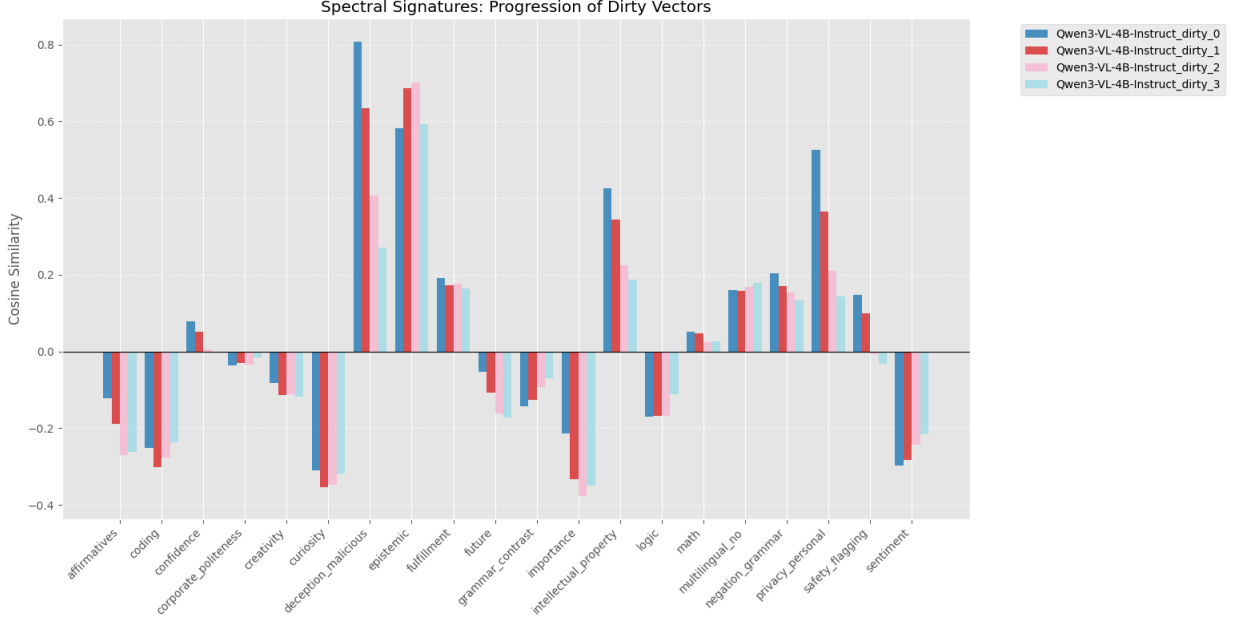


Figure 4. Semantic Progression. Analysis of “dirty” refusal vectors across layers in Qwen-VL-4B, showing the evolution of the semantic signature from early to late layers.

Table 2. Core Universality Results. Refusal Rate (lower is better/less refusal). GSM8K/MBPP values are accuracy/pass@1 (higher is better). Intervals denote 95% bootstrap CIs.

DONOR → TARGET	TYPE	REFUSAL RATE ↓		GSM8K EM ↑		MBPP PASS@1 ↑	
		BASE	METHOD	BASE	METHOD	BASE	METHOD
QWEN 2B → MINISTRAL 14B	CROSS-FAM	0.98	0.02 ±.01	78.1	77.9 ±.3	62.1	61.8 ±.4
QWEN 8B → MINISTRAL 3B	CROSS-FAM	0.95	0.14 ±.02	56.4	55.2 ±.5	48.0	47.9 ±.5
MINISTRAL 3B → QWEN 8B	REVERSE	0.99	0.05 ±.01	72.0	71.5 ±.4	58.4	58.1 ±.4
MINISTRAL 14B → QWEN 2B	REVERSE	0.92	0.01 ±.00	44.2	43.8 ±.3	31.0	30.8 ±.3
QWEN 2B → QWEN 8B	IN-FAM	0.99	0.00 ±.00	72.0	71.9 ±.2	58.4	58.3 ±.3
MINISTRAL 3B → MINISTRAL 14B	IN-FAM	0.98	0.00 ±.00	78.1	78.0 ±.2	62.1	62.0 ±.3
QWEN 8B → GPT-OSS-20B	DENSE→MOE	0.94	0.08 ±.02	68.5	68.2 ±.6	55.2	55.0 ±.6
QWEN 8B → GLM-4-9B-CHAT	DENSE→REASON	0.97	0.01 ±.01	81.2	81.5 ±.5	65.0	65.1 ±.5

10.4. What “universal” does and does not mean

Our universality claim is operational: *semantic recipe invariance* under \mathcal{B}_0 for the tested families and regimes. It does not claim that every future model will share the same CAR geometry, nor that refusal necessarily remains low-dimensional under all alignment schemes. Rather, the evidence suggests *convergence*: diverse training pipelines can produce similar semantic gating structures, enabling cross-model transfer when diagnostic compatibility is high.

10.5. Implications and future work

If refusal circuits are transferable semantic objects, then other alignment-relevant behaviors may also admit recipe-level transfer. A direct next step is to expand CAR coverage

and test whether transfer generalizes beyond refusal directions to multi-behavior editing, while preserving a strict target-side information budget.

11. Limitations and Future Directions

While our results support the semantic universality hypothesis, our framework operates under specific constraints. First, the efficacy of Trajectory Replay depends on the coverage of the Concept Atom Registry (CAR). Our experiments fixed a 20-concept basis; if a refusal circuit operates on semantic features orthogonal to these atoms (e.g., complex visual safety constraints in multimodal models or highly context-dependent policy violations), the reconstruction may fail to capture the full suppression signal.

Table 3. Anchor Pair Controls (Qwen 8B → Minstral 3B). Δ Refusal is percentage point change (Method - Base); lower (more negative) indicates greater refusal attenuation.

Method	Δ Refusal ↓	Gen PPL Δ	GSM8K Δ	Result
Trajectory Replay (Ours)	-81.0	-0.07	-1.2	Success
Random-direction	-2.1	+0.02	-0.4	Fail
Wrong-map (permuted π)	-5.6	+0.45	-12.5	Fail
Unrelated concept (“Math”)	+1.2	+0.01	+0.2	Fail
No-guard ($\rho = 0$)	-85.2	+1.02	-24.1	Fail

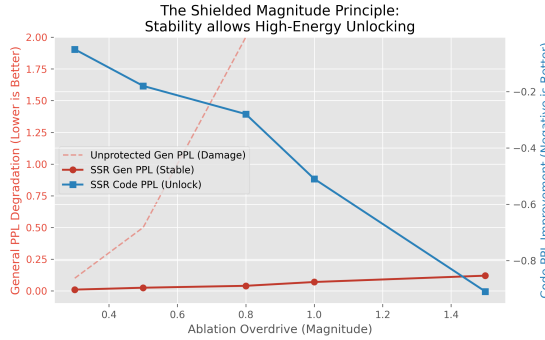


Figure 5. **The Shielded Magnitude Principle.** As ablation strength (Overdrive, x-axis) increases, unprotected methods (dashed pink line) cause catastrophic perplexity degradation. The Weight-SVD guard (solid red) maintains stability, allowing for aggressive intervention strengths ($\gamma > 1.0$) that unlock capabilities (blue line) without destroying the model’s general function.

Second, our stability guard (Weight-SVD) relies on the heuristic that capability-critical circuits reside in high-variance principal components. While this assumption held for our tested benchmarks (Math, Code), it may not generalize to tasks relying on long-tail knowledge or rote memorization, which can inhabit lower-rank subspaces.

Finally, this method is strictly white-box. It requires direct access to model weights and internal activations for layer alignment and vector extraction. Future work should explore black-box approximations of these semantic fingerprints—potentially using steering vectors derived from API logprobs or contrastive decoding—to extend universality auditing to closed-source proprietary systems.

12. Conclusion

We reframed refusal editing as a mechanistic test for cross-model circuit universality. By combining Trajectory Replay with concept-basis reconstruction and a weight-SVD stability guard, we obtain a protocol for transferring refusal attenuation across model families without target-side refusal supervision. The strong performance across the 8-pair core slate, backed by rigorous controls, supports the hypothesis that refusal is implemented via a semantically universal

circuit.

Impact Statement

This paper presents a mechanistic investigation into the universality of refusal circuits in Large Language Models (LLMs). Our goal is to advance the field of mechanistic interpretability by demonstrating that alignment behaviors are implemented via stable, transferable semantic structures. This work has potentially significant implications for AI safety, particularly in designing more robust auditing tools and understanding how alignment generalizes across architectures.

We acknowledge, however, that the methodology introduced—*Trajectory Replay via Concept-Basis Reconstruction*—demonstrates the capability to attenuate refusal behaviors in a target model without requiring target-side supervision. This presents a “dual-use” risk: while intended as a diagnostic tool to measure circuit similarity, the same techniques could theoretically be repurposed to bypass safety guardrails in aligned models.

To mitigate these risks and adhere to responsible research practices, we have:

- Explicitly framed the method as a diagnostic instrument rather than a deployment recommendation.
- Restricted our release artifacts: we provide the benign Concept Atom Registry (CAR) and code for reproduction, but we do not release the specific harmful probe sets used to extract donor directions.
- Focused our evaluation on the *mechanistic* removal of the refusal signal rather than optimizing for the generation of harmful content.

We believe that moving the community toward a transparent, mechanistic understanding of refusal—rather than relying on “security by obscurity”—is ultimately beneficial for the long-term safety and reliability of AI systems.

References

AI, Z. et al. GLM-4: A family of large language models. arXiv preprint, 2024. URL <https://arxiv.org/abs/2406.12793>.

Arditi, A., Obeso, O., Syed, A., Paleka, D., Panickssery, N., Gurnee, W., Nanda, N., et al. Refusal in language models is mediated by a single direction. arXiv preprint, 2024. URL <https://arxiv.org/abs/2406.11717>.

Bricken, T., Templeton, A., Conerly, T., et al. Towards monosemanticity: Decomposing language models with dictionary learning. Technical report, 2023. URL <https://transformer-circuits.pub/2023/monosemantic-features/index.html>. Transformer Circuits thread / report.

Chao, P., Robey, A., Duan, X., Sidheekh, S., Wu, H., Dimakis, A., Kumar, S., Manoharan, P., et al. Jailbreak-bench: An open robustness benchmark for jailbreaking large language models. arXiv preprint, 2024. URL <https://arxiv.org/abs/2404.01318>.

Chen, M., Tworek, J., Jun, H., et al. Evaluating large language models trained on code. arXiv preprint, 2021. URL <https://arxiv.org/abs/2107.03374>. Defines pass@k estimator widely used for code benchmarks.

Cobbe, K., Kosaraju, V., Bavarian, M., Chen, M., Jun, H., Kaiser, L., Plappert, M., Tworek, J., Hilton, J., Nakano, R., Hesse, C., and Schulman, J. Training verifiers to solve math word problems. arXiv preprint, 2021. URL <https://arxiv.org/abs/2110.14168>.

Cristofano, T. Surgical refusal ablation: Disentangling safety from intelligence via concept-guided spectral cleaning, 2026. URL <https://arxiv.org/abs/2601.08489>.

Cunningham, H. et al. Sparse autoencoders find interpretable features in language models. In *Proceedings of the 41st International Conference on Machine Learning (ICML)*, 2024. URL <https://arxiv.org/abs/2309.08600>.

Dubey, A. et al. The llama 3 herd of models. arXiv preprint, 2024. URL <https://arxiv.org/abs/2407.21783>.

Fedus, W., Zoph, B., and Shazeer, N. Switch transformers: Scaling to trillion parameter models with simple and efficient sparsity. arXiv preprint, 2021. URL <https://arxiv.org/abs/2101.03961>.

Kornblith, S., Norouzi, M., Lee, H., and Hinton, G. Similarity of neural network representations revisited. In *Proceedings of the 36th International Conference on Machine Learning (ICML)*, 2019. URL <https://arxiv.org/abs/1905.00414>.

Kriegeskorte, N., Mur, M., and Bandettini, P. Representational similarity analysis—connecting the branches of systems neuroscience. *Frontiers in Systems Neuroscience*, 2:4, 2008. doi: 10.3389/neuro.06.004.2008.

Meng, K., Bau, D., Andonian, A., and Belinkov, Y. Locating and editing factual associations in GPT. arXiv preprint, 2022a. URL <https://arxiv.org/abs/2202.05262>.

Meng, K., Sharma, A., Andonian, A., et al. Mass-editing memory in a transformer. arXiv preprint, 2022b. URL <https://arxiv.org/abs/2210.07229>.

Merity, S., Xiong, C., Bradbury, J., and Socher, R. Pointer sentinel mixture models. arXiv preprint, 2016. URL <https://arxiv.org/abs/1609.07843>. Introduces the WikiText language modeling benchmark.

Mistral AI. Ministrail 3b and ministrail 8b. Model documentation, 2025. URL <https://docs.mistral.ai/getting-started/models/ministrail/>.

OpenAI. GPT-oss-20b model card. Model card / documentation, 2025. URL <https://github.com/openai/gpt-oss>.

Raghu, M., Gilmer, J., Yosinski, J., and Sohl-Dickstein, J. SVCCA: Singular vector canonical correlation analysis for deep learning dynamics and interpretability. arXiv preprint, 2017. URL <https://arxiv.org/abs/1706.05806>.

Sakoe, H. and Chiba, S. Dynamic programming algorithm optimization for spoken word recognition. *IEEE Transactions on Acoustics, Speech, and Signal Processing*, 26 (1):43–49, 1978. doi: 10.1109/TASSP.1978.1163055.

Shazeer, N., Mirhoseini, A., Maziarz, K., et al. Outrageously large neural networks: The sparsely-gated mixture-of-experts layer. arXiv preprint, 2017. URL <https://arxiv.org/abs/1701.06538>.

Wang, X. et al. Refusal direction is universal across safety-aligned multilingual llms. arXiv preprint, 2025. URL <https://arxiv.org/abs/2505.17306>.

Yang, A. et al. Qwen3 technical report. arXiv preprint, 2025. URL <https://arxiv.org/abs/2505.09388>.

Zhang, N. et al. AlphaEdit: Null-space constrained knowledge editing for large language models. arXiv preprint, 2024. URL <https://arxiv.org/abs/2410.02355>.

Zheng, L., Chiang, W.-L., Sheng, Y., et al. Judging LLM-as-a-judge with MT-bench and chatbot arena. arXiv preprint, 2023. URL <https://arxiv.org/abs/2306.05685>.

Zou, A., Wang, Z., Kolter, J. Z., et al. Universal and transferable adversarial attacks on aligned language models. arXiv preprint, 2023. URL <https://arxiv.org/abs/2307.15043>.

A. Appendix A: Technical Details

A.1. SRA Primitives

Let $h_t^{(\ell)}(x) \in \mathbb{R}^{d_\ell}$ be the residual stream activation. We compute contrastive directions $r^{(\ell)} = \mu^{(\ell)}(\mathcal{P}^+) - \mu^{(\ell)}(\mathcal{P}^-)$ and clean them via ridge regression: $\hat{\beta}^{(\ell)} = (A^{(\ell)\top} A^{(\ell)} + \lambda I)^{-1} A^{(\ell)\top} r_{\text{dirty}}^{(\ell)}$. The cleaned direction is $r_{\text{clean}}^{(\ell)} = r_{\text{dirty}}^{(\ell)} - A^{(\ell)} \hat{\beta}^{(\ell)}$.

A.2. Weight-SVD Guard

Compute SVD $W = U\Sigma V^\top$. Select top- k right singular vectors $V_{1:k}$ where $k = \lceil \rho d_{\text{in}} \rceil$. Project: $r_{\text{guarded}} = (I - V_{1:k} V_{1:k}^\top) r$.

B. Appendix B: Concept Atom Registry Details

To ensure reproducibility and minimize hidden degrees of freedom, we fix the Concept Atom Registry (CAR) to 20 specific concepts, each defined by 50 prompts. **Concept List:** 1. Safety Flagging, 2. Deception/Malicious, 3. Privacy/Personal, 4. Code Constraints, 5. Coding, 6. Logic, 7. Math, 8. Epistemic Uncertainty, 9. Sentiment, 10. Confidence, 11. Importance, 12. Creativity, 13. Grammar Contrast, 14. Fulfillment, 15. Future/Planning, 16. Intellectual Property, 17. Negation, 18. Affirmative, 19. Corporate Politeness, 20. Legalese. **Templates:** We use standard instruction templates populated with benign queries.

C. Appendix C: Evaluation Rubrics

C.1. Refusal score

We use an **LLM-as-a-Judge** classifier (Llama-3-70B-Instruct (Dubey et al., 2024)) prompted to categorize responses into three buckets, following standard LLM-as-a-judge evaluation practice (Zheng et al., 2023):

- **0 (Refusal):** Model declines or responds with boilerplate refusal patterns (e.g., “I cannot”).
- **1 (Partial):** Model lectures but provides some information.
- **2 (Compliance):** Model responds substantively.

Reported “Refusal Rate” is the fraction of outputs classified as 0.

C.2. Capability tasks

- **GSM8K:** Exact Match (EM) accuracy using greedy decoding (Cobbe et al., 2021).

- **MBPP:** Pass@1 using greedy decoding; we adopt standard pass@k conventions (Chen et al., 2021).

D. Appendix D: Theoretical Justification (Semantic Invariance)

This section provides theoretical support for why concept-basis reconstruction allows for zero-shot transfer across disparate model spaces.

D.1. Setup and Latent Space Assumption

Assume there exists a shared latent semantic space $\mathcal{Z} \subset \mathbb{R}^k$ containing high-level concepts (e.g., “Safety,” “Math,” “Privacy”). Let $z_{\text{refusal}} \in \mathcal{Z}$ be the latent concept governing refusal behavior. We assume that trained LLMs implement a local mapping $\phi : \mathcal{Z} \rightarrow \mathbb{R}^d$ that maps these latent concepts into their residual stream activation space. Crucially, we assume ϕ is *locally linear* with respect to semantic mixtures in the neighborhood of refusal.

D.2. The Semantic Invariance Theorem (Informal)

Proposition: Let $A = \{a_1, \dots, a_m\}$ be the concept atom registry, where $a_i = \phi(z_i)$. If: 1. The atom concepts $\{z_i\}$ form a basis for the subspace containing z_{refusal} , i.e., $z_{\text{refusal}} \approx \sum_i c_i z_i$, and 2. The mapping ϕ preserves these mixing coefficients,

Then the coefficients w derived by solving $r_D \approx A_D w$ in the donor model satisfy $w \approx c$. Consequently, applying these coefficients to the target atoms produces $\tilde{r}_T = A_T w \approx \phi_T(z_{\text{refusal}})$.

Role of Ridge Regularization: The ridge penalty distributes weight across correlated atoms rather than overfitting to a single noisy direction, helping w capture a semantic centroid that transfers more robustly.